

# Sustained feedback-induced oscillations in a hybrid single mode semiconductor plasmonic laser

D. Cui, J. Chen, A. Bousseskou, H. Huang, and F. Grillot

**Abstract**—This work investigates the response to external optical feedback of a hybrid plasmonic semiconductor laser. Intensity noise measurements revealed the relaxation oscillation frequency whereas tabletop feedback experiments unveil a stronger reflection immunity, with a significant margin of 8 dB in comparison with a standard semiconductor laser made with a dielectric waveguide. On the top of that, the hybrid plasmonic laser does not exhibit a typical route to chaos but rather sustained induced-feedback oscillations instead. These results reveal new properties of hybrid plasmonic semiconductor lasers and provide guidelines in designing laser sources for on-chip hybrid plasmonic integrated platform.

**Index Terms**—Surface plasmon, distributed feedback laser, optical feedback

## I. INTRODUCTION

Integrated photonics has become a lot of attraction over the past decades. By miniaturizing an entire optical bench-top onto a single chip, photonic integrated circuits (PICs) provide sophisticated functionalities for various fields such as remote sensing, biomedical analysis, structural health monitoring, but most commonly, PICs are heavily promoted in optical communication applications. Nowadays, high-performance, PIC-based devices are commercially available on the market, hence offering unparalleled compactness, high cost- and energy-efficiency, as well as extensive bandwidth capacity. On the other hand, to achieve high bandwidth density, it is necessary to accommodate both photonic and electronic integrated circuits (EICs) in close proximity. On this stage, one limiting factor is the conventionally employed dielectric waveguide. Due to the diffraction limit, the width of standard dielectric waveguides must be on the same order than the operating wavelength of the lightwave propagating within namely  $\geq \lambda/n$ , with  $\lambda$  being the wavelength and  $n$  the waveguide refractive index [1]. In addition, it is known that the bending radius of the waveguides cannot be reduced below the micrometer scale without suffering from heavy loss [2], [3]. Therefore, one attractive approach to shrink down the optical circuitry

relies on using plasmonic technology. Plasmonics deals with electromagnetic waves coupled to charge oscillations on metal-dielectric interfaces, namely the so-called surface plasmon polaritons (SPPs). SPPs can be seen as a virtual particle resulting directly from the interaction of light and free electrons on a metal surface that is limited near the metal-dielectric interface and providing a strong light confinement in the near field [4]. Thanks to the conductor skin effect, SPPs are surface-bounded [5], thus, with proper design and fabrication, sub-wavelength waveguides, commonly referred as plasmonic waveguides, can be exploited to replace conventional dielectric structures in order to operate below the diffraction limit. In the view of developing high-speed photonics with plasmonic technology, it is also crucial to study the integration of plasmonic waveguides with other building-blocks namely with laser sources, modulators, detectors, etc. On this front, plasmonic-based modulators and detectors with outstanding performance were already reported in recent studies [6], [7]. Over the past two decades, plasmonic-based spasers i.e., surface plasmon amplification by stimulated emission of radiation) and nanolasers were also demonstrated [8]. However, the realization of such nano light-emitters require delicate fabrication procedures. Besides, the attenuation of SPPs being significant, operating threshold and output power are quite limited in such nanodevices. which limit their utilization in practice. To overcome the problem, low-dimensional semiconductor nanomaterials such as those based quantum dots can also be considered to provide sufficient material gain to compensate for metal-induced losses [9]. In this work, we study another configuration relying on a hybrid plasmonic semiconductor laser. As described hereinafter, the hybrid mode stems from the coupling between a classical polarized mode guided and a SPP mode. Therefore, it has much lower loss compared to the pure plasmonic mode in metals at the 1D one-dimensional periodic gold nanowire arrays on top of a dielectric waveguide [10] and sandwich-type structure of high index nanowire/low index spacer/metal nanolaser at telecommunication wavelengths [11]. Here, we investigate the noise and nonlinear response of a hybrid plasmonic distributed feedback (DFB) laser device that takes advantage of the existing and mature quantum-well (QW) technology. In particular, we explore the optical feedback dynamics, which is of paramount importance for PIC applications wherein external reflections may quickly accumulate from different inner interfaces, therefore affecting the laser source. Tabletop experiments were carefully set up to and all results are compared with a commercialized QW DFB laser made with a conventional dielectric waveguide. Intensity noise measurements reveal a resonance frequency whereas

Manuscript created November, 2022;

D. Cui is with LTCI, Télécom Paris, Institut Polytechnique de Paris, 91120 Palaiseau, France (di.cui@telecom-paris.fr).

H. Huang is with LTCI, Télécom Paris, Institut Polytechnique de Paris, 91120 Palaiseau, France.

J. Chen is with LTCI, Télécom Paris, Institut Polytechnique de Paris, 91120 Palaiseau, France.

A. Bousseskou is with the Center of Nanosciences and Nanotechnologies (C2N), University Paris-Saclay 91120 Palaiseau, France.

F. Grillot is with the Center for High Technology Materials, University of New Mexico, Albuquerque, NM 87106 USA, and also with LTCI, Télécom ParisTech, LTCI, Télécom Paris, Institut Polytechnique de Paris, 91120 Palaiseau, France (e-mail:frederic.grillot@telecom-paris.fr).

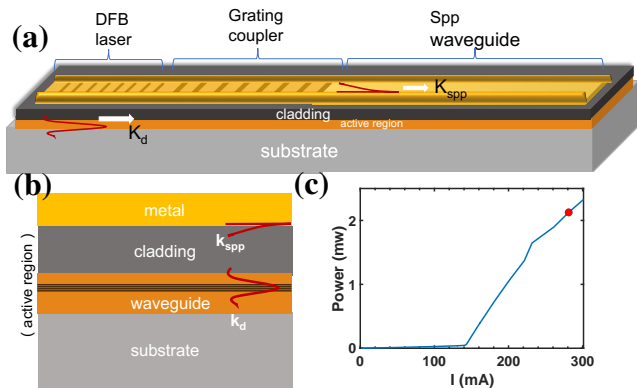


Fig. 1. (a) The schematic of full integrated plasmonic device. (b) The cross-section showing both the SPP mode (top) and hybrid mode (bottom) propagating into the waveguide structure.  $k_d$  is the wavevector of the guided mode.  $k_{spp}$  is the wavevector of the surface plasmon polariton. (c) The light-current characteristic measured at 15 °C.

feedback experiments unveil a stronger reflection immunity, along with sustained periodic oscillations in comparison with the reference QW laser. These results bring novel insights in semiconductor lasers incorporating plasmonic structure which is meaningful for on-chip hybrid plasmonic integrated platforms.

## II. LASER STRUCTURE, STATIC AND INTENSITY NOISE

Fig. 1(a) depicts the complete structure of an integrated hybrid plasmonic DFB laser source, which consists of a DFB laser, the grating coupler and a SPP waveguide. In this geometry, the grating in the DFB section makes the laser single mode whereas the grating coupler adapts the wave vectors, and allows for an efficient SPP launching into the waveguide. It basically diffracts a part of the waveguided mode, hence its period must be chosen in order that constructive interference takes place into the SPP mode. In this work, we focus on the nonlinear gain properties when subjected to optical feedback, therefore only the DFB laser section is considered, and the corresponding epilayer structure is schematically presented in Fig. 1(b). The active region consists of 300 nm made with nine 10-nm tensile-strained InGaAlAs quantum wells (QWs), grown by metal-organic vapor phase epitaxy (MOVPE) on n-doped substrate. A thin cladding layer of 450 nm is developed on top for two purposes: providing sufficient refractive index contrast for light confinement and a charge reservoir for the p-n junction. The surface of the cladding is then coated with a 70-nm-thick (3 nm Ti, 67 nm Au) metallic strip that includes the DFB grating patterned by using electrical-beam lithography followed by lift-off the metal layer deposited with electron-beam evaporation. The laser cavity length measures 360  $\mu\text{m}$  in length, with cleaved facets on both side. Further details of the material aspects can be found in these references [12]. The schematic in Fig. 1(b) shows the dielectric mode and SPP mode in the laser cavity. Semiconductor lasers for telecommunications typically operate in transverse electric (TE) polarization owing to tensile strained QW. However, a transverse magnetic (TM) polarization can also be obtained

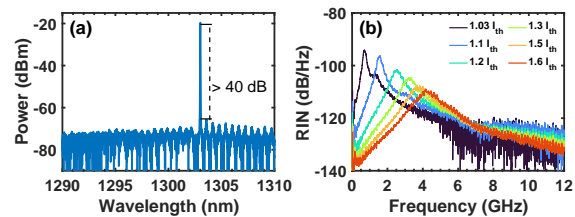


Fig. 2. Optical spectrum of the hybrid plasmonic DFB laser.(a) Measured laser output power as a function of lasing wavelength at  $2 \times I_{th}$  ( $\sim 294$  mA, red marker in Fig. 1(c))

(b)Relative intensive noise (RIN) spectrum of the hybrid plasmonic DFB laser under different bias currents at 15 °C.

thanks to the strain. SPPs are transverse magnetic (TM) polarized, therefore strained QWs represent an excellent candidate as gain material for surface plasmon amplification [12].

The hybrid mode is a mixture between the plasmonic mode  $k_{spp}$  in the metal layer and the photonic mode  $k_d$  in the DFB waveguide. In other words, the hybrid mode stems from the coupling between a classical TM polarized mode  $k_d$  guided within the active region by the dielectric claddings and a surface plasmon mode  $k_{spp}$  guided at the interface between the upper cladding and the top metal contact of the device, as the interpretation in the cross-sectional view of Fig. 1(a). The coupling strength between the two components depends on the materials index, the ridge width, and can be tuned with the upper cladding thickness which is here fixed to 450 nm. Near-field optic experiments already demonstrated the correspondence of the gold/semiconductor interface with the plasmonic component of the hybrid-mode [12].

Static characterizations of the laser device are performed under continuous-waves (CW) at 15 °C. The light-current characteristics (LI) is presented in the Fig. 1(c), the threshold current  $I_{th}$  is measured at 141 mA. This high value is the direct consequence of the metal loss on the surface. The red dot on the LI curve at  $2 \times I_{th}$  marks where the optical spectrum in Fig. 2 (a) is captured. The DFB mode is located around 1303 nm, and the side mode suppression ratio (SMSR) exceeding 40 dB indicating that the laser is perfectly single mode with a very good control of amplified spontaneous emission.

Fig. 2(b) shows the relative intensity noise (RIN) of the hybrid plasmonic laser at 15 °C and under different bias currents ranging from  $1.03 I_{th}$  to  $1.6 \times I_{th}$ . The evolution of the RIN is pretty much similar to what is commonly observed in conventional devices with a minimum RIN level of -135 dB/Hz within the measured range. [13]. The experiments unveil the relaxation oscillation frequency of the hybrid laser which varies from 0.6 GHz near threshold up to 4 GHz at  $1.6 \times I_{th}$ . However, at low bias, the resonance appears to be sharper than in standard device. Although this effect needs to be further investigated, it may be attributed to the additional contribution from the SPP wave which leads to a lower damping during the laser operation. We also studied the linewidth enhancement effect of the DFB laser that is associated to the phase-amplitude coupling effect. In order to measure the linewidth enhancement factor ( $\alpha_H$ ), the amplified spontaneous emission

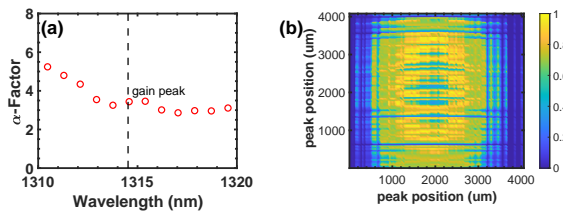


Fig. 3. (a) The measured  $\alpha_H$ -factor from of a hybrid plasmonic FP laser sharing the material properties than the hybrid plasmonic DFB laser. The value of  $\alpha_H$  at gain peak (grey dash line) is  $\sim 3.1$ . (b) The mode profile measured using Scanning-Slit Optical Beam Profilers at  $2 \times I_{th}$ .

method is employed. In spite of its practicality, this method is only adequate for multimode configuration, therefore, a hybrid plasmonic Fabry-Perot laser having the same active region than the hybrid plasmonic DFB laser was considered. Fig. 3 (a) the spectral dependence of the  $\alpha_H$  at threshold. At gain peak, it is found of 3.1 which is similar to what was reported in plasmonic nanolasers [14]. Finally, the mode profile was also measured using Scanning-Slit Optical Beam Profilers at  $2 \times I_{th}$ . As shown in Fig. 3 (b), the beam is found more elliptical than in conventional lasers. Together these considerations do influence the feedback sensitivity. While the former must be minimized, it is also important to stress that the smaller the beam divergence, the higher the optical power feedback into the active region.

### III. OPTICAL FEEDBACK EXPERIMENTS

The optical feedback experiments are performed within the long-cavity regime. The fiberized external cavity is 10 meters in length which corresponds to an external round-trip time of 100 ns. The feedback strength  $r_{ext}$  is defined as the ratio between the reflected power that reached the laser cavity on the output DFB facet left-as cleaved and the free space power emitted from the same facet. In our tabletop experiment, the achievable  $r_{ext}$  ranges from -73 dB up to -21 dB, with the consideration of the losses in fibers and at the coupling. Further details of the experimental setup can be found elsewhere [15]. The top two maps (Fig. 4(a) and 4(b)) displays the optical and RF spectral maps of the hybrid plasmonic device as  $r_{ext}$  increases, while the lower two (Fig. 4(c) and 4(d)) give those of the dielectric based QW DFB laser. The colorbar distinguishes the spectral intensity at a given wavelength/frequency and feedback strength.

At low feedback  $r_{ext} < -40$  dB, the lasing mode of both lasers remain steady without visible modal broadening, nor any sign of nonlinear oscillations being excited. Above  $r_{ext} > -35$  dB, the noise of the reference DFB starts growing at a frequency of 5.5 GHz (Fig. 4(d)), which is attributed to the undamping of the relaxation oscillations. Thereafter, at -40.5 dB optical feedback strength, the laser reaches the critical feedback level  $r_{crit}$  (marked by a vertical dashed orange line in every maps) which corresponds to the maximum feedback value that can be tolerated by a communication system [15]. Beyond  $r_{crit}$ , periodic oscillations arise in the RF domain, then the lasing optical modes broaden hence leading to a fully

chaotic operation at large feedback levels ( $r_{ext} > -30$  dB). In the case of the hybrid plasmonic DFB laser, the response to optical feedback is found different in particular without clear route to chaos. We estimated the critical feedback level at -33 dB. When  $r_{ext}$  goes beyond that value, optical adjacent modes start to intensify around the lasing modes along with an additional frequency contribution at twice the ROF (10 GHz). At higher feedback ( $r_{ext} > -25$  dB), as the beating in the RF spectral map of the hybrid plasmonic laser is progressively widened, optical side modes remain still visible in the corresponding optical spectral map, implying that the nonlinear dynamics maintained sustained periodic oscillations, while the spectral profiles of the reference laser in both optical and RF domain have emerged into single, largely broadened envelopes. This window of periodic oscillations, where RF spectra exhibit a narrow peak sustained from the ROF expands over 8 dB for the hybrid plasmonic device under study against 2 dB for the reference QW DFB laser.

In order to confirm the absence of chaotic operating in the hybrid plasmonic laser, Figure 4(e) and (f) compare the RF spectra at maximal feedback amount of -21.5 dB, i.e. on the right edge of the maps in Fig. 4(b) and 4(d), to the RF spectra in free running for both lasers. In Fig. 4(e), the envelope is well centered around 5 GHz, with the presence of the second harmonic around 10 GHz. It can also be noticed that, the background noise of the feedback spectrum is on the same level as in free-running, hence, it is reasonable to conclude that, chaotic oscillations are not present at  $r_{ext} = -21.5$  dB. On the other hand, when the dielectric based QW laser is subjected to the same amount of feedback, the RF spectral profile exhibits clear signatures of the chaotic behaviors: a large -3 dB bandwidth that exceeds 12 GHz, and a lifted background noise up to 10 dB above free-running spectrum.

Despite a quite large  $\alpha_H$  factor, these comparisons demonstrate that the hybrid plasmonic device has a feedback tolerance about 8 dB higher than the standard device. Indeed, the losses in the plasmonic waveguide can be considered as a related factor in attenuating the reflections. Moreover, the TM polarization of the emission from plasmonic laser is an important feature as well. In ideal setting, when a TM wave is reflected by a mirror, the field takes an opposite sign compared to the incident one, thus the two contra-propagative waves can establish destructive interference that further attenuate the external reflection, which is different compared to the TE-polarized light in the reference laser. As aforementioned, the large beam divergence may also somewhat counteract the large phase-amplitude coupling effects [16]. On the other hand, the sharpened relaxation oscillation shown in Fig. 2 that are enhanced by the SPPs, may impede the formation of irregular and complex dynamics. The cladding between the waveguide and the active region may as well act as a buffer capacity, preventing drastic carrier density variation induced by external reflection in the gain medium. For the perspective of photonic integration, these nonlinear properties can be exploited to generate stable arbitrary RF frequency with reliable signal-to-noise ratio. Consequently, feedback experiments unveil a stronger reflection immunity in comparison with a standard semiconductor laser made with a dielectric waveguide.

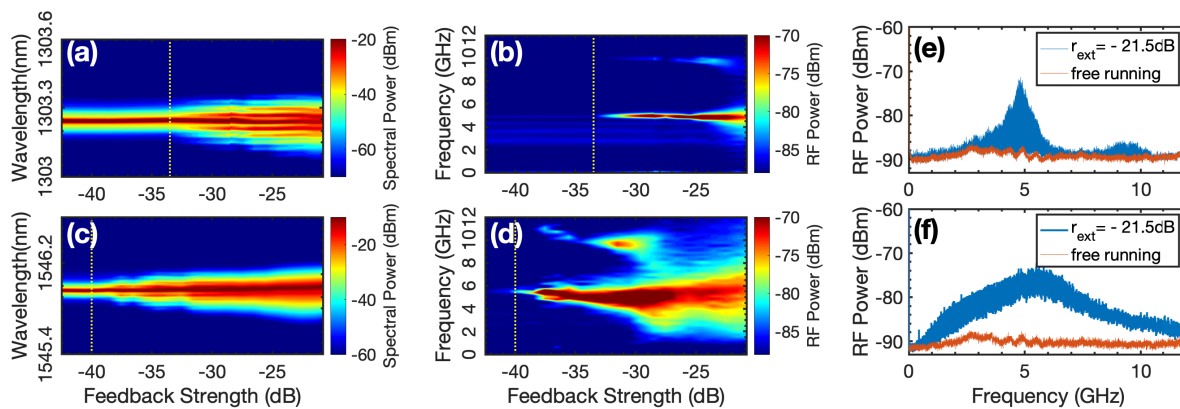


Fig. 4. (a) Optical spectral maps for hybrid plasmonic QW DFB laser and (c) dielectric based QW DFB laser; RF spectral maps for (b) hybrid plasmonic QW DFB laser and (d) dielectric based QW DFB laser. Both lasers are biased at  $2 \times I_{th}$ . RF spectra of (e) hybrid plasmonic QW DFB laser and (f) dielectric QW laser in free running (blue) and under maximal optical feedback (orange), measured at  $2 \times I_{th}$ .

#### IV. CONCLUSIONS

In this work, we studied nonlinear properties of a hybrid plasmonic QW DFB laser operating in the telecommunication band subjected to optical feedback. It is very instructive for the general understanding of feedback induced instabilities. Experimental investigation is then extended to verify if chaos state is indeed hard to be established in hybrid plasmonic devices when subjected to optical feedback. In presence of optical feedback, experiments demonstrated that, compared to a standard QW DFB device, the plasmonic one exhibits a much wider window of periodic oscillations. One contributing factor to this finding is attributed to the unusually underdamped relaxation that may result from the surface plasmon waveguide. Theoretical investigations is also continued in order to establish the validity of the present hypotheses. Overall, these results bring novel insights into laser sources fully compatible with plasmonic integration platform, and contribute to the conception of innovative plasmonic devices for ultra-fast signal processing and high-volume datacom [17], [18].

#### ACKNOWLEDGMENTS

The authors acknowledge Dr. D. Costantini from Saint-Gobain Recherche France. Di CUI's work is also supported by China Scholarship Council.

#### REFERENCES

- [1] J. Takahara, S. Yamagishi, H. Taki, A. Morimoto, and T. Kobayashi, "Guiding of a one-dimensional optical beam with nanometer diameter," *Optic Letters*, vol. 22, no. 7, pp. 475–477, 1997.
- [2] M. Cherchi, S. Ylino, M. Harjanne, M. Kapulainen, and T. Aalto, "Dramatic size reduction of waveguide bends on a micron-scale silicon photonic platform," *Optic Express*, vol. 21, no. 15, pp. 17814–17823, Jul 2013.
- [3] A. Brimont, X. Hu, S. Cuffe, P. Rojo Romeo, G. Saint Girons, A. Griol, A. Zanzi, P. Sanchis, and R. Orobthchouk, "Low-Loss and Compact Silicon Rib Waveguide Bends," *IEEE Photonics Technology Letters*, vol. 28, no. 3, pp. 299–302, 2016.
- [4] L. Salomon, F. Grillot, A. Zayats, and F. de Fornel, "Near-Field Distribution of Optical Transmission of Periodic Subwavelength Holes in a Metal Film," *Physical Review Letters*, vol. 86, no. 6, pp. 1110–1113, 2001.
- [5] W. L. Barnes, A. Dereux, and T. W. Ebbesen, "Surface plasmon subwavelength optics," *Nature*, vol. 424, no. 6950, pp. 824–830, 2003. [Online]. Available: <https://doi.org/10.1038/nature01937>
- [6] M. Burla, C. Hoessbacher, W. Heni, C. Haffner, Y. Fedoryshyn, D. Werner, T. Watanabe, H. Massler, D. L. Elder, L. R. Dalton, and J. Leuthold, "500 GHz plasmonic Mach-Zehnder modulator enabling sub-THz microwave photonics," *APL Photonics*, vol. 4, no. 5, p. 056106, 2019.
- [7] Y. Salamin, P. Ma, B. Baeuerle, A. Emboras, Y. Fedoryshyn, W. Heni, B. Cheng, A. Josten, and J. Leuthold, "100 GHz Plasmonic Photodetector," *ACS Photonics*, vol. 5, no. 8, pp. 3291–3297, 2018.
- [8] S. I. Azzam, A. V. Kildishev, R.-M. Ma, C.-Z. Ning, R. Oulton, V. M. Shalaev, M. I. Stockman, J.-L. Xu, and X. Zhang, "Ten years of spasers and plasmonic nanolasers," *Light: Science & Applications*, vol. 9, no. 1, p. 90, May 2020.
- [9] P. Berini and I. De Leon, "Surface plasmon–polariton amplifiers and lasers," *nature photonics*, vol. 2, pp. 16–24, 2008.
- [10] A. Christ, S. Tikhodeev, N. Gippius, J. Kuhl, and H. Giessen, "Waveguide-plasmon polaritons: strong coupling of photonic and electronic resonances in a metallic photonic crystal slab," *Physical review letters*, vol. 91, no. 18, p. 183901, 2003.
- [11] R. F. Oulton, V. J. Sorger, D. Genov, D. Pile, and X. Zhang, "A hybrid plasmonic waveguide for subwavelength confinement and long-range propagation," *Nature Photonics*, vol. 6, no. 8, pp. 16–, 2012.
- [12] D. Costantini, "Generation and amplification of surface plasmon polaritons at telecom wavelength with compact semiconductor-based devices," Ph.D. dissertation, Université Paris Sud-Paris XI, 2013.
- [13] L. A. Coldren, S. W. Corzine, and M. L. Mashanovitch, *Diode lasers and photonic integrated circuits*. John Wiley & Sons, 2012.
- [14] P. Ginzburg and A. V. Zayats, "Linewidth enhancement in spasers and plasmonic nanolasers," *Opt. Express*, vol. 21, no. 2, pp. 2147–2153, Jan 2013.
- [15] J. Duan, H. Huang, B. Dong, D. Jung, J. C. Norman, J. E. Bowers, and F. Grillot, "1.3- $\mu\text{m}$  Reflection Insensitive InAs/GaAs Quantum Dot Lasers Directly Grown on Silicon," *IEEE Photonics Technology Letters*, vol. 31, no. 5, pp. 345–348, 2019.
- [16] F. Grillot, J. C. Norman, J. Duan, Z. Zhang, B. Dong, H. Huang, W. W. Chow, and J. E. Bowers, "Physics and applications of quantum dot lasers for silicon photonics," *Nanophotonics*, vol. 9, no. 6, pp. 1271–1286, 2020.
- [17] Y. Salamin, B. Baeuerle, W. Heni, F. C. Abrecht, A. Josten, Y. Fedoryshyn, C. Haffner, R. Bonjour, T. Watanabe, M. Burla, D. L. Elder, L. R. Dalton, and J. Leuthold, "Microwave plasmonic mixer in a transparent fibre-wireless link," *Nature Photonics*, vol. 12, no. 12, pp. 749–753, Dec 2018.
- [18] M. Eppenberger, A. Messner, B. I. Bitachon, W. Heni, T. Blatter, P. Habegger, M. Destraz, E. De Leo, N. Meier, N. Del Medico, C. Hoessbacher, B. Baeuerle, and J. Leuthold, "Resonant plasmonic micro-racetrack modulators with high bandwidth and high temperature tolerance," *Nature Photonics*, vol. 17, no. 4, pp. 360–367, Apr 2023.